

Numerical and analytical solution of stresses on a box-type lining structure under the effect of ground fracture

W Huang^{1, 2}, D Y Liu^{1, 2, 3*}, H F Jiang^{1, 2}, F Y Liu^{1, 2}

¹College of Civil Engineering, Chongqing University, Chongqing, China, 400045

²Key Laboratory of New Technology for Construction of Cities in Mountain Area (Chongqing University) Ministry of Education, Chongqing, China, 400045

³School of Civil Engineering and Architecture, Chongqing University of Science & Technology Chongqing, Chongqing, China, 401331

Received 5 April 2014, www.tsi.lv

Abstract

This study attempts to study the stress mechanism of a box-type lining structure during its inclined penetration of ground fissure and calculate the normal stress and shearing stress of the structure section. Based on thin-wall structure theory combined with the stress boundary conditions of the physical model of the box-type lining structure, we derived the analytical solution of the normal stress and shearing stress of the physical model. The stress analytical solution indicates that the damage of the footwall of the ground fissure is more serious than that of the hanging wall, which could match the physical model experiment. The effectiveness and accuracy of the analytical solution of the normal stress and shearing stress of the section were verified using finite element software to establish the mechanical model of the box-type lining structure. The results of the numerical model were compared with the analytical solution results.

Keywords: Box-type structure, Lining structure, Ground fissure, Analytical solution

1 Introduction

Xi'an City, China is one of the cities with the most intensely developed ground fractures in the world. When the box-type lining structure of the subway in Xi'an penetrates the active ground fracture, the tunnel structure becomes subject to the bending stress and shearing stress under the pressure of the surrounding rocks. This condition is caused by the faulting of the hanging wall and the heading wall of the ground fracture. The normal rate of the vertical movement of the ground fracture in the area is 5 to 35 mm/a , whereas the maximum rate is 55.06 mm/a [1]. The intense ground fissure movement threatens the subway operation. At the same time, the current designing codes do not cover the stress design of the section of the integral box-type lining structure, and no code could be followed for the designing of the project [2].

With the development of underground space in the 20th century, tunnelling technology has witnessed rapid development. Rich experiences have been accumulated in terms of ground fissure research [3], stress analysis of tunnel structures [4-9], and the construction of subway tunnels [10]. Pavlovic et al. [11] conducted a numerical simulation on the bending and torsion performance of a thin-wall box-type column to analyse the influence of the initial fault and residual stress on the bending stability. Park et al. [12] conducted an on-site survey and material

test to analyse the damage caused by a fire accident to the box-type subway tunnel in Daegu City, South Korea and propose a remedy plan. Stirbys et al. [13] used structural processing measures, such as expanding section and the combination of solid support and flexible support, to resolve the issues encountered during the penetration of the tunnel through the faults.

Although other researchers [14, 15] have exposed the cause of the formation of the ground fissures in Xi'an and the analytical solution of the torsional deformation [16], studies on the analytical solution of the bending and shearing stresses on the integral box-type lining structure when penetrating through active ground fissures are rare.

This study focuses on the disaster-causing mechanism of active ground fractures over box-type subway tunnels and decreasing the disastrous effect of the ground fractures on the subway operation. We have deduced the analytical solution of the bending and shearing stresses of an integral box-type lining structure during the inclined penetration through active ground fractures. We have also established a finite element model to analyse the bending and shearing deformations of the box-type structure to provide theoretical and model references for the subway structure designing in ground fracture areas. The results can help to enrich the knowledge on the stress influence of subway structures crossing ground fracture sections.

* Corresponding author email: liudy@cuq.edu.cn

2 Model Stress Analysis

2.1 MODEL OVERVIEW

The foundation settlement test platform is used to establish the physical model of the integral box-type lining structure penetrating ground fractures according to a ratio of similitude of 1:5. The disturbed soil (silty clay)

of the actual stratum in Xi'an is used for the test. The ground fracture is imitated by filling with silty-fine sand with a dip angle of 85°, which intersects with the axes of the structure at 30°. The major physico-mechanical indexes could basically meet the similarity relation. Figure 1 shows the section of the soil layers. Reference 1 lists the detailed settings of the physical model.

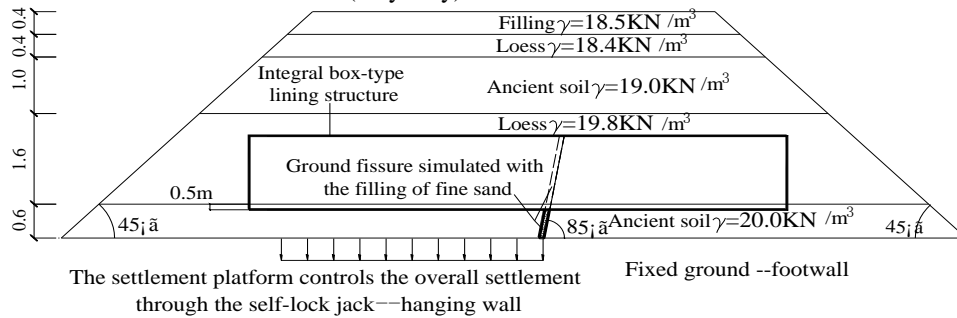


FIGURE 1 Physical model of integral box-type lining structure

2.2 BOUNDARY CONDITIONS OF MODEL STRESS

The section centreline dimension of the integral box-type lining structure was $d_1 \times d_2 = 1182\text{mm} \times 1090\text{mm}$, the wall thickness was $d = 120\text{mm}$, the structural length of the physical model was 10 m, and the ground fracture was 6 m away from the left end of the structure. During the test, the heading wall of the ground fracture was fixed, and the settlement of the ground fracture was simulated with the operation rate and movement of the self-lock jack installed on the hanging wall of the ground fracture. With the relative lowering of the hanging wall of the ground fracture, an empty space was formed at the bottom of the hanging wall. According to the available test results, the basal contact pressure of the maximum earth pressure cell was zero within 0 to 0.5 m from the heading wall to the ground fracture because the lining structure is subject to bending deformation. With the increase in the settlement, the contact pressure at the bottom of the hanging wall on the left end surface of the lining structure gradually decreased to zero. This condition indicates that the empty space at the bottom of

the lining structure has expanded to the entire bottom of the heading wall with the increase in the settlement.

According to the observations of the physical model test, the boundary conditions of the lining structure could be concluded as follows. The top of the box-type lining structure was under the pressure load from the uniformly distributed soil P. This condition subjected the structure to the bending and shearing damages at the empty space of the hanging wall and the local area near the ground fracture at the heading wall Figure 2. The left end surface of the lining structure was buried in the fourth and fifth filling layers Figure 1. Its movement in the axial direction X was smaller than the movement of the empty space along the vertical direction Z. Thus, the left end surface of the lining structure was considered as the directional supporting base Figure 2. The right end surface of the lining structure was on the heading wall that was relatively fixed, which was also buried in the fourth and fifth layers of the soil Figure 1. Thus, the right end surface of the lining structure could be considered as the fixed supporting base Figure 2.

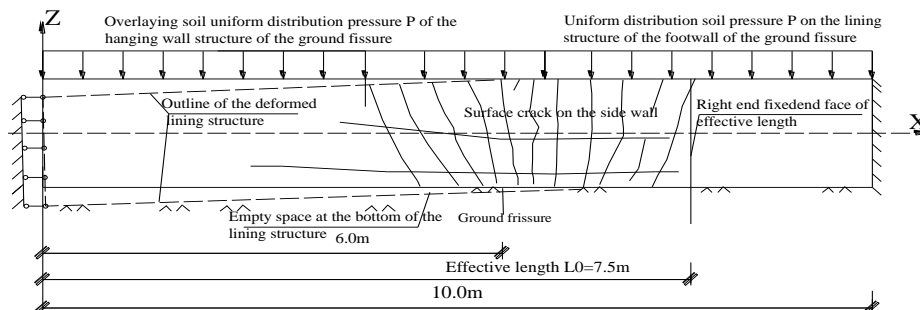


FIGURE 2 Stress Diagram of Integral Box-Type Lining Structure

3 Analytical Solution of the Bending and Shearing Stresses of the Box-Type Lining Structure

3.1 FUNDAMENTAL ASSUMPTIONS

(1) Given the wall thickness ($d = 120\text{mm}$) is smaller than the width of the section and the length of the structure, the shearing stress flow generated from the

shearing deformation is assumed to be uniformly distributed along the wall thickness.

(2) The plane cross-section assumption is used in calculating the bending deformation of the integral box-type lining structure.

(3) In the physical model, the ground fracture is 6 m away from the left end surface of the structure, whereas the overall length of the integral box-type lining structure is 10 m. Given that the bottom of the box-type lining structure was subject the maximum bending deformation within 0 to 0.5 m of the heading wall of the ground fracture, the soil body at the bottom collapsed to move downward and form an empty space. Thus, the scope of the empty space was $x=0\sim 6.5\text{m}$, whereas the right end of the structure's effective length was fixed within

$x=6.5\sim 10.0\text{m}$. According to the test results, the effective length of the box-type lining structure is assumed to be $L_0=7.5\text{m}$ Figure 2.

3.2 BENDING NORMAL STRESS OF THE INTEGRAL BOX-TYPE LINING STRUCTURE

According to the fundamental assumptions, the integral box-type lining structure was subject to the bending stress over the effective length of $L_0=7.5\text{m}$ under the overlying uniform distribution soil pressure P . The cross-sections that are vertical to the axes of the tunnel Figure 3a were still plane after the structure bended, and were vertical to the axes of the deformed lining structure.

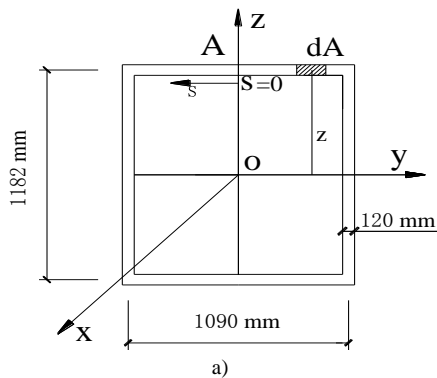


FIGURE 3 Cross Section of the Integral Box-Type Lining Structure

Figure 3a) shows a cross section of the box-type lining structure. $o-xyz$ is a rectangular coordinate system crossing the section centroid of the section, whereas $o-x$ is the axis of the lining structure. The intersection point of axis $o-z$ and the middle surface of the structure is A , s is the curve coordinate of the outline of the middle surface of the structure, and the anti-clockwise direction is the positive direction. A is the initial point of the curve coordinate s . The wall thickness was $d = 120\text{mm}$.

According to the plane cross-section assumption, the normal strain at any arbitrary point on the section is as follows:

$$\varepsilon_x = \frac{z}{\rho}, \tag{1}$$

where ρ is the curvature radius of the neutral layer of the section, and z is the vertical distance between any point and the neutral layer.

The normal stress of the section is as follows:

$$\sigma_x = \frac{Ez}{\rho}. \tag{2}$$

According to the torque equilibrium equation surrounding axis y :

$$M_y = \int_A \sigma_x z dA. \tag{3}$$

Placing (2) into (3) achieves the following:

$$M_y = \int_A \frac{E^2}{\rho} dA = \frac{E}{\rho} I_y. \tag{4}$$

Placing (4) into (2) achieves the following:

$$\sigma_x = \frac{M_y}{I_y} z \tag{5}$$

where M_y is the bending moment surrounding axis y on section x , and I_y is the moment of inertia surrounding axis y .

3.3 SHEARING STRESS OF THE INTEGRAL BOX-TYPE LINING STRUCTURE

Considering that, the integral box-type lining structure is relatively fixed at the footwall, its part at the hanging wall moves downward. Each section of the lining structure is subject to the shearing stress caused by the overlying soil pressure P . Suppose a unit $ds \times dx$ with a thickness of $d = 120\text{mm}$ at the initial point of the coordinate s Figure 4.

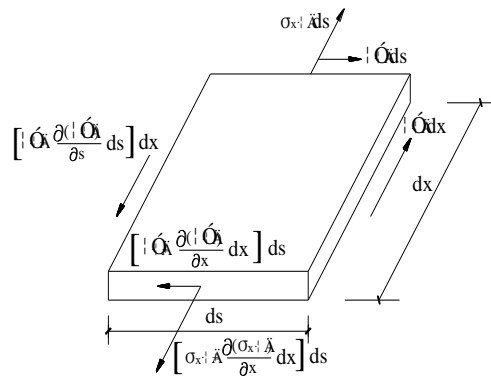


FIGURE 4 Axial Projection Drawing of the Side-Wall Stress of the Structure

Given that $\sum x = 0$:

$$\frac{\partial(\sigma_x \delta)}{\partial x} + \frac{\partial(\tau \delta)}{\partial s} = 0. \tag{6}$$

Considering that the wall thickness $d = 120\text{mm}$ is constant to irrelevant to x , thus:

$$\tau \delta = -\int_0^s \delta \frac{\partial \sigma_x}{\partial x} ds + C_1(x). \tag{7}$$

Placing (5) and the shear $Q_z = \partial M / \partial x$ at the direction z into (7), and assuming the shearing stress flow $q = \tau \delta$, then:

$$q = q_0 + q_A = -\left(\frac{Q_z}{I_y} S_y\right) + (\tau \delta)_A, \tag{8}$$

where $q_A = (\tau \delta)_A$ is the shearing stress flow of the initial point A of the curvilinear coordinates of the section.

We have introduced the continuous conditions [17, 18] $\oint u(x, s) ds = 0$ of the warping movement of the section of the box-type lining structure. These conditions are set to $u(x, s)$ as the axial warping displacement of the section x coordinate to calculate the axial warping displacement of point s in the section through the shear deformation $du / ds = \gamma = q / (G\delta)$.

$$u(x, s) = \int_0^s \frac{q}{G\delta} ds + u_A. \tag{9}$$

The integral initial point of formula (9) is point A . From the initial point A , the line integral is conducted along the outline of the section to A . The relative axial displacement is zero. Thus:

$$u - u_A = \oint \frac{q}{G\delta} ds = 0. \tag{10}$$

Placing (8) into (10) achieves the following:

$$q_A = -\oint \frac{Q_z}{\delta I_y} S_y ds / \oint \frac{ds}{\delta}. \tag{11}$$

Placing (11) into (4) achieves the section shearing stress flow:

$$q = q_0 + q_A = \frac{Q_z}{I_y} (-S_y + \frac{\oint S_y ds}{\oint \frac{ds}{\delta}}), \tag{12}$$

where Q_z is the shear in the direction z on section x , S_y is moment of area of point s related to axis y , and $d = 120\text{mm}$ is the wall thickness of the section.

4 Analytical Solution of the Bending Normal Stress and Shearing Stress of the Integral Box-Type Lining Structure

4.1 SOLUTION TO THE BENDING NORMAL STRESS OF THE SECTION

According to the abovementioned boundary conditions and fundamental assumptions, the following factors are determined. The effective length of the integral box-type lining structure was $L_0 = 7.5\text{m}$. The left end surface of the structure is the directional supporting base. The right end surface is the fixed supporting base. The distance between the ground fracture and the left end surface was 6 m. The overlaying uniform distribution soil pressure was $p = 0.065\text{MPa}$, whereas the linear load along the axes of the lining structure was $q = 0.065 \times 1210 = 78.65\text{kN/m}$. The bending moment (which makes the tension on the lower part of the section and the pressure on the upper part of the section positive) and the shear (Table 1) of each $L/15$ section are calculated.

According to (1), $I_y = 0.125735089\text{m}^4$ and $z = 0.591\text{m}$. The maximum bending normal stress of each $L/15$ section of the box-type lining structure could be then calculated Table 1.

TABLE 1 Maximum Normal Stress and Shearing Stress of the Integral Box-Type Lining Structure Section

Section Location	Bending Moment M_y	Shearing Stress Q_z	Maximum Normal Stress of the Analytical Method	Maximum Normal Stress of the Numerical Method	Maximum Shearing Stress of the Analytical Method	Maximum Shearing Stress of the Numerical Method
	kN*m	kN	MPa	MPa	MPa	MPa
0	737.625	0.0	3.467	3.617	0.000	0.000
L/15	452.238	39.325	2.126	2.214	0.155	0.151
2L/15	186.794	78.650	0.878	0.954	0.311	0.319
3L/15	-58.988	117.975	-0.277	-0.203	0.466	0.487
4L/15	-285.106	157.300	-1.340	-1.584	0.621	0.654
5L/15	-491.563	196.625	-2.311	-2.547	0.777	0.822
6L/15	-678.356	235.950	-3.189	-3.406	0.932	0.990
7L/15	-845.4875	275.275	-3.974	-4.289	1.088	1.158
8L/15	-992.956	314.600	-4.667	-4.863	1.243	1.321
9L/15	-1120.763	353.925	-5.268	-5.487	1.398	1.494
10L/15	-1228.906	393.250	-5.776	-5.972	1.554	1.661
11L/15	-1317.388	432.575	-6.192	-6.411	1.709	1.829
12L/15	-1386.206	471.900	-6.516	-6.766	1.864	1.997
13L/15	-1435.363	511.225	-6.747	-6.951	2.020	2.165
14L/15	1464.856	550.550	-6.885	-7.214	2.175	2.332
L	1474.688	589.875	-6.932	-7.481	2.330	2.500

4.2 SOLUTION TO THE SHEARING STRESS OF THE SECTION

The linear load of the lining structure along the axes was $q=78.65kN/m$. The left end surface of the structure model was the directional supporting base, whereas the right end surface was the fixed supporting base. Thus, the shear Q_z on each $L/15$ section of the structure could be calculated. The maximum shearing stress of each $L/15$ section Table 1 could be calculated by placing the above shear Q_z into (12), which occurs halfway the height of the section.

5 Finite Element Model

The 3D finite element model of the integral box-type lining structure was established according to the severe of the soil layer shown in Figure 5. This model verifies the maximum normal stress and shearing stress of the section obtained through the analytical method.

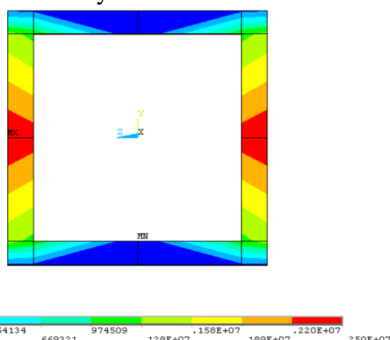


FIGURE 5 Diagram of the Shearing Stress on the Right End Section Surface

The BEAM188 structure unit to simulate the box-type lining structure, which is in contact with the interfaces set for the soil layers, was considered. The left end surface of the lining structure was set as the directional supporting base, whereas the right end surface was set as the fixed

supporting base. According to the actual settlement, the hanging wall of the ground fissure was gradually decreased to 20cm in the software. Table 1 shows the maximum normal stress and shearing stress of each section $L/15$ calculated at the final settlement of 20cm. Figure 5 shows the maximum normal stress and the shearing stress of the right end surface of the structure.

6 Conclusion

The analytical solution of the normal stress and shearing stress of the bending deformation of an integral box-type lining structure passing through ground fractures has been calculated. This solution is based on the physical model test and boundary conditions (i.e., the left end is the directional supporting base, whereas the right end is the fixed supporting base). The conclusions and suggestions of this study are as follows:

- (1) With the lowering of the hanging wall of the ground fracture and the formation of the empty space, the lower side of the section of the lining structure (0~2L/15) was subject to the tension. The upper side of the 3L/15~L section was subject to the tension. The maximum normal stress along the axes of the structure increased gradually. At the right end section, the normal stress reached a maximum value of 6.932MPa, which is significantly larger than the standard strength of extension of C30 concrete.
- (2) The maximum section shearing stress of the integral box-type lining structure is subject to linear increase along the axes and reaches the maximum value at the right end section. The maximum shearing stress is achieved at halfway the height of the section.
- (3) The maximum normal stress and shearing stress on the section of the heading wall of the ground fracture (12L/15) are larger than those of the hanging wall. During the bending of the structure, the ring-direction cracks

could be seen on the heading wall section first. The damage to the heading wall because of the bending is more serious than that to the hanging wall.

(4) The damage effect of the integral box-type lining structure is large when passing through ground fractures. Special deformation joints are set to release the stresses on the structure near the ground fractures. Water proof measures also need to be taken.

References

- [1] Ji Y S 2009 *Model test study on the interaction of subway tunneling and surrounding rock in ground fissure* Master Thesis of Chang'an University, China.
- [2] Huang W 2011 *Study on analytic solution of torsional deflection on subway tunnel structure inclined wear activities ground fissure* Master Thesis of Chang'an University, China.
- [3] Liu L, Chen L Q, Tang J X 2010 Present Situation and Future Prospects of Geologic Environment Issues in Mines in China *Disaster Advance* 3(4) 563-6
- [4] Stirbys A F, Radwanski Z R, Proctor R J 1999 Los Angeles metro rail project-geologic and geotechnical design and construction constraints *Engineering Geology* 51(3) 203-24
- [5] Pavlovic L, Froschmeier B, Kuhlmann U 2012 Finite element simulation of slender thin-walled box columns by implementing real initial conditions *Advances in Engineering Software* 44(1) 63-74
- [6] Ling D S, Guo H G, Wu J 2012 Research on seismic damage of metro station with centrifuge shaking table model test *Journal of Zhejiang University (Engineering Science)* 46(12) 2202-9
- [7] Skee A, Bjelanovic G, Jelenic G 2013 Glued timber-concrete beams-analytical and numerical models for assessment of composite action *Engineering Review* 33(1) 41-49
- [8] Wang S R, Chang M S 2012 Reliability Analysis of Lining Stability for Hydraulic Tunnel under Internal Water Pressure *Disaster Advance* 5(4) 166-70
- [9] Kultasov K A, Rysbekova A A 2012 Calculation of composite plates of variable thickness and fold in action radial force *Computer Modelling & New Technologies* 16(3) 54-57
- [10] Duan B F, Li L 2012 Grouting Reinforcement Technique for Subsurface Excavation of Group Metro Tunnels Construction in Complex Environment *Disaster Advance* 5(4) 1508-12
- [11] Pavlovic L, Kuhlmann U, Froschmeier B 2012 Finite element simulation of slender thin-walled box columns by implementing real initial conditions *Advances in Engineering Software* 44(1) 63-74
- [12] Park S Y, Oh H H, Shin Y S 2006 A case study on the fire damage of the underground and its repair works *Tunnelling and Underground Space Technology* 21(3) 328
- [13] Stirbys A F, Radwanski R Z, Proctor R J, Escandon R F 1999 Los Angeles metro rail project-geologic and geotechnical design and construction constraints *Engineering Geology* 51(3) 203-24
- [14] Peng J B, Hu Z P, Men Y M 2009 Test study of deformation and damage mechanism of horseshoeshaped tunnel crossing ground fissure with 40° *Chinese Journal of Rock Mechanics and Engineering* 28(11) 2258-65 (in Chinese)
- [15] Fan W, Deng L S, Peng J B 2008 Study of the physical model experiment of subway tunnel crossing the ground fissure belt *Chinese Journal of Rock Mechanics and Engineering* 27(9) 1917-23 (in Chinese)
- [16] Liu D Y, Huang W, Luo L J, Li D S, Zhao B Y 2013 Torsion deformation's analytic solution of box tunnel crossing ground fissure *Journal of Civil, Architectural & Environmental Engineering* 35(1) 1-6 (in Chinese)
- [17] Huang J Y 1998 *The torsion analysis of thin-walled structure - The curve beam and diagonal branch box beam* China Railway Publishing House: Beijing (in Chinese)
- [18] Zhang Y H 2008 Study on shear stress of thin-walled member with closed section under restrained torsion *Journal of Lanzhou Jiaotong University* 27(4) 1-3 (in Chinese)

Acknowledgements

This work was funded by the National Natural Science Foundation Funding Project (Grant Nos. 40602033 and 41302223) and the Chongqing City Fundamental and Advanced Research Projects (cstc2013jcyjA90004).

Authors	
	<p>Huang W, born in April, 1984, College of Civil Engineering, Chongqing University, Chongqing, P.R. China</p> <p>Current position, grades: Doctor of College of Civil Engineering, Chongqing University, China. University studies: BEng. in College of Civil Engineering from Chang'an University in China. ME Civil Engineering from Chang'an University in China. Scientific interest: Geotechnical Engineering, Underground Structure. Publications: 5 papers published in various journals. Experience: 5 scientific research projects.</p>
	<p>Liu D Y, born in October, 1959, College of Civil Engineering, Chongqing University, Chongqing, P.R. China</p> <p>Current position, grades: Professor of Civil Engineering, Chongqing University, China. University studies: BEng from Chengdu university of Science & Technology in China. D.E. from Chongqing University in China. Scientific interest: Geotechnical Engineering, Underground Structure Publications: 120 papers published in various journals. Experience: 20 scientific research projects.</p>
	<p>Jiang H F, born in December, 1982, College of Civil Engineering, Chongqing University, Chongqing, P.R. China</p> <p>Current position, grades: Doctor of College of Civil Engineering, Chongqing University, China. University studies: BEng in College of Civil Engineering from Chongqing Jiaotong University in China. ME Civil Engineering from Chongqing Jiaotong University in China. Scientific interest: Geotechnical Engineering. Publications: 6 papers published in various journals. Experience: 6 scientific research projects.</p>
	<p>Liu F Y, born in December, 1989, College of Civil Engineering, Chongqing University, Chongqing, P.R. China</p> <p>Current position, grades: the Master of College of Civil Engineering, Chongqing University, China. University studies: BEng in College of Civil Engineering from Chongqing University in China. Scientific interest: Geotechnical Engineering, Underground Structure Publications: 3 papers published in various journals. Experience: 2 scientific research projects.</p>